

Depth Driven Photometric and Geometric Image Registration for Real-Time Stereo Systems

W. Waizenegger¹, I. Feldmann¹ and P. Eisert^{1,2}

¹Fraunhofer Institute for Telecommunications, Heinrich Hertz Institute, Berlin, Germany

²Humboldt University, Berlin, Germany

Abstract

This paper presents a novel depth driven approach for a highly accurate joint photometric and geometric image alignment. Thereby, the registration problem is expressed in terms of a consistent, elegant and efficient energy formulation. Moreover, we propose a real-time capable alternating iterative optimization scheme to solve for a state of minimal energy. Since our energy formulation is based on pixel wise color similarity our registration procedure directly improves the performance of disparity estimation and the visual quality of multi-view view synthesis.

Categories and Subject Descriptors (according to ACM CCS): Photometric and Geometric Registration, Real-Time, Stereo, 3D Video Processing, GPGPU

1. Introduction

A careful adjustment of image colors is advantageous and vital for many multi-view computer vision algorithms. Among other, computational stereo and a constitutive view synthesis can greatly benefit from high precision photometric alignment. According to the exhaustive studies of Hirschmüller et al. [HS09], [HS07] disparity estimation results for a stereo image pair recorded with the very same camera, i.e. identical photometric settings, tend to be superior to those taken with different color adjustments. But even with a careful manual balancing of all camera settings for a stereo system, it is difficult and time consuming to adapt and match photometric properties off all cameras. While a sophisticated color chart based manual photometric adjustment is possible under lab conditions, there are many application that do not allow intricated user interaction. Particularly, user centric on-line stereo systems, like eye contact preserving video-communication solutions, as depicted in figure 1, require a fully automatic color registration work-flow, cf. [SFA*08], [WASF11], [WFS11].

In this work, we propose a novel depth driven algorithm for high accuracy joint geometric and photometric stereo image registration. The goal is to optimize photometric camera settings with respect to optimal depth estimation results. We simultaneously aim at the fully automatic on-line adjustment

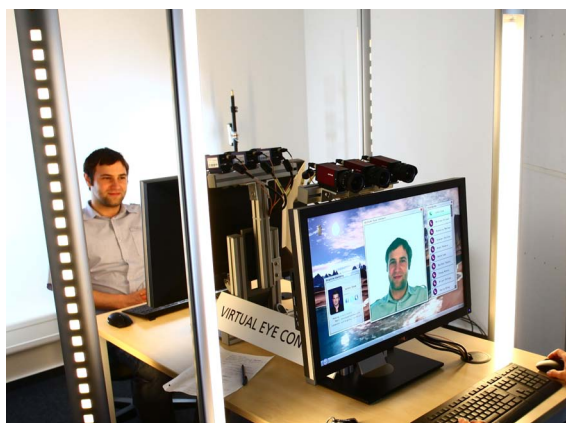


Figure 1: An eye contact preserving video-communication research system. Based on depth estimation a virtual view is synthesized. To enable acceptable visual quality for a multi-view view synthesis the different images need to be photometrically aligned.

of colorimetric camera settings and at the electronic off-line fine-tuning of photometric properties for recorded stereo sequences. The registration process is formulated in terms

of an alternating energy minimization procedure, where the geometric and photometric registration energies are consistently incorporated into the same continuous energy functional. This allows us to use the powerful machinery of the variational calculus in order to optimize for a state of minimal energy. Moreover, since we pursue a depth based geometric image registration and the photometric registration concurrently, the quality of photometric registration is directly related to the performance of depth estimation and vice versa. Therefore, our approach is perfectly suited to enhance the outcome of stereo algorithms and improve the visual experience of a resulting view-synthesis. Considering real-time stereo systems, where the computational load is of significant interest, matching photometric properties can greatly help to reduce the computational complexity. Instead of specialized and expensive similarity measures that compensate for different radiometric conditions, much simpler similarity measures and smaller window sizes could be used while results of comparable quality can be expected, cf. [HS09], [HS07], [HLL08], [WYD07]. Our registration method is designed with focus on parallelizability which allows for an efficient real-time implementation on graphics hardware using CUDA.

The paper is organized as follows. In section 2 we briefly review related work on the field of photometric and geometric image registration. Section 3 covers the general formulation of our depth driven registration approach in terms of energy minimization. Subsequently, section 4 and 5 introduce the concrete continuous energy functional and the steps for geometric and photometric image registration respectively. In section 6 the fusion of both steps into an alternating iterative minimization scheme is described. Section 7 illustrates the successful implementation of our technique to two different fields of application.

2. Related Work

Photometric and geometric image registration for various applications including aerial photography, image mosaicing or computational stereo has a long tradition in computer vision. Considering stereo vision, one of the key interests is the improvement of matching quality. Beside algorithmic developments for radiometric insensitive similarity measures [HLL08], [WYD07] and intensive studies on the effects of photometric changes to various matching criteria [HS09], [HS07] the improvement of image formation and colorimetric pre-processing has a high focus in in research. While some authors concentrate on a general perspective on digital image formation and parametric color models for digital imaging, e.g. [RSYD05] or [CSZ09] respectively, others take care about concrete algorithmic solutions to perform a full radiometric camera calibration or pursue a normalization approach with respect to lighting geometry and illumination color [KP08], [KFP08], [GN03], [FSC98]. Contrary, there are activities on the development of color chart based auto-

matic image registration methods, e.g. [KSP*10], [IW05]. A more close approach to the work in this paper was proposed by Bartoli [Bar08]. However, in contrast to our work the author focuses on photometric and geometric image registration for post-processing and only performs a highly constrained geometric image registration by homography fitting of the image planes.

3. Image Registration in Terms of Energy Minimization

From a general viewpoint, we define our geometric and photometric stereo registration algorithm as a minimization problem with respect to the following energy

$$E(u, T) := E_S(u) + \lambda E_D(u, T), \quad (1)$$

where the total energy E is a composition of a *smoothness* term E_S and a *data* term E_D weighted by a scalar $\lambda > 0$. The variables u and T denote the geometric and photometric registration functions, respectively. For simplicity, we assume in our work that the stereo image pair is in a rectified state, which can be accomplished by image rectification transformation or sophisticated on-line camera adjustment techniques, e.g. [ZMEK10]. Therefore, neglecting photometric registration and supposing color constancy, for a stereo image pair I, J an optimal geometric registration $u : \Omega \rightarrow \mathbb{R}$ has to fulfill

$$I(\mathbf{x}) = J(x + u(\mathbf{x}), y), \quad (2)$$

where $\mathbf{x} = (x, y)^T$ are Cartesian coordinates in the image domain $\Omega \subset \mathbb{R}^2$, and an image I is considered as a mapping $I : \Omega \rightarrow \mathbb{R}^m$, $I(\mathbf{x}) := (I^{c_1}(\mathbf{x}), \dots, I^{c_m}(\mathbf{x}))$ from Ω to a m -dimensional color space. Finally, we define the photometric registration $T : \mathbb{R}^m \times \mathbb{R}^k \rightarrow \mathbb{R}^m$, with $T(I(\mathbf{x}), \mathbf{p}) = (T^{c_1}(I(\mathbf{x}), \mathbf{p}), \dots, T^{c_m}(I(\mathbf{x}), \mathbf{p}))$ as a color transformation mapping with a k -dimensional parameter vector $\mathbf{p} = (p_1, \dots, p_k)$. Rewriting equation (2) with respect to photometric registration leads to the very basic requirement for a joint geometric and photometric stereo image registration mapping:

$$I(\mathbf{x}) = T(J(x + u(\mathbf{x}), y), \mathbf{p}). \quad (3)$$

In the following, we will compose a concrete continuous energy formulation according to the form of equation (1). It takes equations (2) and (3) into consideration and allows for an elegant, consistent and effective joint estimation of the unknown geometric registration function u and the parameter vector \mathbf{p} , for an arbitrary color transformation mapping.

4. Globally Optimal Geometric Image Registration

Based on the general description in section 3, we are now able to motivate the choice of an energy functional that allows a globally optimal solution of the geometric image registration mapping u . Disregarding the photometric registration, based on equation (2), we can derive the commonly

used absolute differences

$$AD(u, \mathbf{x}, I, J) = \sum_{i=c_1}^{c_m} \left| I^i(\mathbf{x}) - J^i(x + u(\mathbf{x}), y) \right| \quad (4)$$

as a pixel wise measure for image registration quality. Consequently, we employ the integral of the absolute differences over the image domain as the *data* term of our energy functional. For regularization, i.e. as a *smoothness* term, we use the total variation of u , which is a convex function that allows sharp discontinuities. Therefore, the minimization task with respect to the unknown geometric registration function can be expressed in terms of the variational problem

$$\min_u \left\{ \int_{\Omega} |\nabla u(\mathbf{x})| + \lambda AD(u, \mathbf{x}, I, J) d\mathbf{x} \right\}. \quad (5)$$

A stationary point for this variational problem could be obtained by solving the corresponding Euler-Lagrange equations with a simple gradient descent approach. However, since the *data* term of the functional cannot be expected to be convex, a stationary point of the functional might be not the globally optimal solution of the variational problem. Additionally, gradient descent iteration approaches suffer from a low rate of convergence.

For our work, we choose another solution for solving the variational problem (5) which was proposed in [PSG*08]. The authors pursue a convexification of the original expression via functional lifting. This allows the computation of a globally optimal solution with an efficient primal-dual proximal point iteration algorithm. Moreover, the algorithm is well suited for parallelization on graphics hardware, which enables the real-time computation of a globally optimal solution for our optimization problem. Especially, considering a video sequence with little changes from one frame to another, the algorithm converges after a few iteration, because the primal and dual variables of the previous frame can be reused for the initialization of the iteration process for subsequent frame.

5. Depth Driven Photometric Image Registration

In the following, we will discuss the algorithmic steps of our photometric registration algorithm in case of a given depth or equivalently a given disparity based geometric registration mapping u . As stated in section 3, we assume a general application specific, parametric color transformation function T with the parameter vector \mathbf{p} to act as the color distortion model. Consequently, we will formulate an energy functional with respect to the considerations of equation (3) and provide a generic iterative minimization scheme for arbitrary color distortion models. Finally, some application specific examples for concrete color transformation mappings and resulting minimization algorithms are presented.

For our photometric registration approach, we choose an

energy functional that is consistent with the geometric registration process in section 4. Therefore, we introduce the color mapping T to the formulation of the minimization task of equation (5) and obtain the optimization problem

$$\min_{\mathbf{p}} \left\{ \int_{\Omega} |\nabla u(\mathbf{x})| + \lambda AD(u, \mathbf{x}, I, T(J, \mathbf{p})) d\mathbf{x} \right\}. \quad (6)$$

Because of preconditioning factors such as auto white balance or almost equal camera default settings, we can expect that the identity mapping is already close to the solution state. Therefore, we rely on a steepest gradient approach for optimizing toward a state of minimal energy. Since $AD(\cdot)$ is not differentiable at 0 we use the differential of the Huber norm with some small constant ϵ

$$H_{\epsilon}'(x) = \begin{cases} \frac{x}{\epsilon} & 0 \leq |x| \leq \epsilon \\ \text{sign}(x) & \epsilon < |x| \end{cases} \quad (7)$$

for the numerical optimization. Clearly, the integration operation of equation (6) does not depend on the optimization variable \mathbf{p} . Thus, denoting $\alpha_i := H_{\epsilon}'(I^i(\mathbf{x}) - T^i(J(x + u(\mathbf{x}), y), \mathbf{p}))$, the gradient of the energy functional with respect to \mathbf{p} reads as follows:

$$\frac{\partial E}{\partial \mathbf{p}} = -\lambda \sum_{i=c_1}^{c_m} \int_{\Omega} \alpha_i \left(\frac{\partial T^i}{\partial p_1}, \dots, \frac{\partial T^i}{\partial p_k} \right)^T d\mathbf{x}. \quad (8)$$

Accordingly, the parameter update of our time marching numerical scheme has the form

$$\mathbf{p}_{n+1} := \mathbf{p}_n - \Delta \frac{\partial E}{\partial \mathbf{p}}, \quad (9)$$

where Δ denotes the applied time step. The repetition of the parameter update until convergence, i.e. until the decrease of energy from n to $n + 1$ drops below a certain threshold, finally leads to the desired solution of the optimization problem (6).

5.1. Example: On-Line White Balance Registration (RGB Translation)

For the setup of a stereo camera pair, a very basic task in order to gain a good photometric matching between the cameras is white balancing. Instead of adjusting each camera separately, our work enables a coupled approach, where the settings of one camera are automatically registered to the other camera. A potential approach for white balancing in digital camera processing pipelines is to transform RGB values to YUV color space, perform white balance by additive modification of U and V channels and transform back to RGB. An appropriate mathematical model for this procedure would be

$$T(r, g, b, u, v) = \mathbf{D} \left(\mathbf{D}^{-1} \begin{pmatrix} r \\ g \\ b \end{pmatrix} + \begin{pmatrix} u \\ v \end{pmatrix} \right), \quad (10)$$

where r, g, b are the values of the red, green and blue color channel, u, v are the white balancing offsets and \mathbf{D} is the

3×3 constant matrix that maps YUV to RGB. Considering equation (8) and (9) the gradient decent optimization with respect to $\mathbf{p} = (u, v)^T$ can be concretely formulated as

$$\mathbf{p}_{n+1} := \mathbf{p}_n + \Delta\lambda \sum_{i=1}^3 \int_{\Omega} \alpha_i \begin{pmatrix} d_{i2} \\ d_{i3} \end{pmatrix} d\mathbf{x}, \quad (11)$$

where $\mathbf{p}_0 = (0, 0)^T$ and $d_{jk}, 1 \leq j, k \leq 3$ denotes the element in the row j and column k of \mathbf{D} . Please note, that the updated parameters can be directly applied to readjust the camera settings.

5.2. Example: Lighting Adjustment (Affine RGB Mapping)

In case of an unknown color distortion function resulting from different lighting conditions a more general mapping should be provided. Clearly, a sophisticated lighting model could be approximated, cf. [KP08], [KFP08], but as we will show in section 7.3 the application of the affine RGB mapping

$$\mathbf{T}(r, g, b, \text{vec}(\mathbf{A})^T, \mathbf{t}^T) = \mathbf{A} \begin{pmatrix} r \\ g \\ b \end{pmatrix} + \mathbf{t} \quad (12)$$

within our framework leads to decent results as well. The variable \mathbf{A} denotes an arbitrary 3×3 matrix, $\text{vec}(\cdot)$ the row wise vectorization operator and \mathbf{t} a translation vector in RGB space. Consequently, the update of the parameter vector $\mathbf{p} = (\text{vec}(\mathbf{A})^T, \mathbf{t}^T)^T$ reads as

$$\mathbf{p}_{n+1} := \mathbf{p}_n + \Delta\lambda \int_{\Omega} \begin{pmatrix} \mathbf{V} & \mathbf{0} & \mathbf{0} \\ \mathbf{0} & \mathbf{V} & \mathbf{0} \\ \mathbf{0} & \mathbf{0} & \mathbf{V} \\ 1 & 0 & 0 \\ 0 & 1 & 0 \\ 0 & 0 & 1 \end{pmatrix} \begin{pmatrix} \alpha_1 \\ \alpha_2 \\ \alpha_3 \end{pmatrix} d\mathbf{x}, \quad (13)$$

where $\mathbf{V} = \mathbf{J}^T(x + u(\mathbf{x}), y)$, $\mathbf{0} = (0, 0, 0)^T$ and the initial parameter vector is the identity mapping $\mathbf{p}_0 = (1, 0, 0, 0, 1, 0, 0, 0, 1, 0, 0, 0)^T$.

6. Joint Photometric and Geometric Image Registration

Considering sections 4 and 5, it can be expected that the geometric image registration results benefit from a given, precise photometric image registration mapping and vice versa. Therefore, we propose to merge both procedures into a joint alternating iterative minimization scheme. Each iteration cycle consists of a small fixed number of iterations to solve for u and one iteration to solve for \mathbf{p} . Figure 2 provides a high level schematic illustration of our depth driven registration pipeline. The input for the registration process is an on-line or recorded stereo image pair or video stream, where the second image is transformed according to the application specific color distortion function. Based on the input image pair, the geometric registration is performed as outlined in section 4. However, instead of iterating until convergence, we only conduct a small fixed number of primal-dual proximal point iterations in order to allow for a joint convergence

of geometric and photometric registration. Thereby, we can avoid photometric registration biases caused through the interdependency of both registration processes. Afterwards, we store the intermediate primal and dual variables of the proximal point iteration as initial values for the next input stereo pair and pass a geometrically registered version of the second image to the photometric registration step. There, an update of the color transformation parameter vector of the application specific color distortion model is computed and handed over to the input module in order to update the color transformation mapping for the second image. Depending on the actual use case, the parameter update can be applied to an electronic transformation mapping for off-line processing or directly for the adjustment of camera interface parameters in an on-line setup. Subsequently, the entire procedure is repeated with updated color transformation parameters until the joint convergence of both registration steps. Formally we define the converged state of our algorithm as the drop of energy reduction from one iteration to the next below a certain threshold.

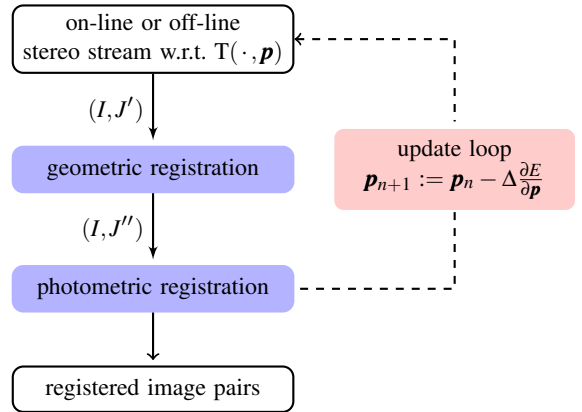


Figure 2: General schematic illustration of our registration algorithm. The image pair (I, J') , where $J' = T(J, \mathbf{p})$ is subject to geometric registration optimization in the first step. In the second step photometric registration is applied to (I, J'') with $J''(\mathbf{x}) = J'(x + u(\mathbf{x}), y)$. A feedback loop takes care about the color adjustment of the input images.

7. Experimental Results

In the following, we demonstrate the performance of our registration algorithm for two different kinds of applications and three different datasets. Section 7.1 compares the application of our method to consistent multi-view white balancing with an individual gray card based manual approach. Section 7.2 evaluates the white balancing performance of our algorithm with a professionally recorded and photometrically adjusted stereo video sequence that is considered as ground truth. Finally, section 7.3 discuss the correction for

different lighting conditions for an image pair of the Middlebury *Aloe* dataset.

7.1. Video-Communication with Virtual Eye Contact

In standard monocular point to point video-communication systems the conferees usually look at the screen while being recorded from a camera beside or above the display. One possibility to preserve eye contact is to use more than one camera, perform a 3D scene analysis and render a synthetic view for a camera which is located at the position of the screen where the conferee is looking at, cf. [SFA*08], [WASF11], [WFS11]. Because of occlusions it is beneficial to use texture information from different cameras for view synthesis. However, user acceptance is directly linked to a good photometric alignment. In the following, we present the results of a typical setup for the eye contact preserving video-communication system depicted in figure 1 which is equipped with three synchronized AVT Pike 210C firewire cameras.

The system setup requires a consistent white balance for all cameras. To illustrate the advantages of our registration algorithm we compare a carefully performed manual color adjustment with our proposed method. Although we rely here on off-line results, please note that our algorithm allows a fully automatic, real-time and on-line color registration which is of great importance for video-communication applications.

In figure 3, results of a manual gray card based individual white balancing for two cameras are illustrated. It can be seen that the image pair suffers from clearly visible color deviations. Moreover, the left image of figure 4 shows that view synthesis based on these input images leads to visually unpleasant results. The outcome after a post-processing according to the proposed joint white balance adjustment in section 5.1 is illustrated in the right image of figure 4. In contrast to the synthesis based on the manually configured color settings the automatically registered synthesis does not possess visual discomfort.

7.2. 3D Video

In recent years, the movie industry and television broadcasters got raising interest in 3D video acquisition technology. The correct and consistent alignment of photometric properties among cameras is of great importance for this field of application. In the following, we use a professionally recorded and photometrically aligned high definition (HD) stereo sequence as ground truth dataset for the evaluation of our registration process. For this purpose, we synthetically introduce a wrong white balancing as illustrated in figure 5. After a correction according to section 5.1 the impact on view synthesis is shown in figure 6. It can be clearly seen that the results for the uncorrected image contain an unpleasant color transition while despite the originally huge color differences



Figure 3: Results for a manual gray card based individual white balancing. There are clearly visible color deviations.

there is no recognizable color border in the corrected version. Moreover, the mean relative numerical error for the estimated color transformation parameter vector is significantly below one percent which proves that our registration algorithm converged to the original state. Finally, as it is of great interest for view generation for 3D displays we illustrate the impact on disparity estimation obtained during the geometric image registration step. As depicted in figure 7, the quality of disparity estimation remarkably improves after the joint photometric and geometric registration procedure.

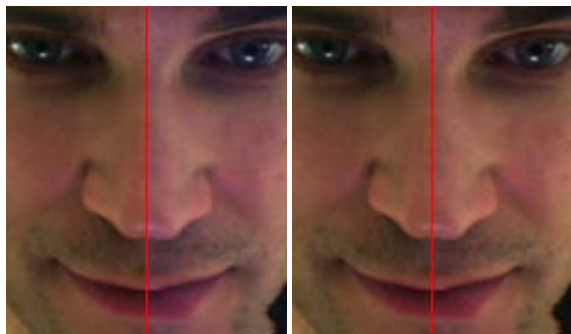


Figure 4: Two closeups of view synthesis based on the scene in figure 3. Both syntheses are composed from the left image of figure 3 on the left of the red line and from the right image on the right of the red line. The left synthesis is performed from the original colors and the right after a post-processing with our registration algorithm.



Figure 5: Left and right image of a professionally recorded and photometrically aligned stereo sequence. Top: Original left image. Bottom: Right image with a synthetic wrong white balancing.

7.3. Middlebury Stereo

In the following, we demonstrate the correction for different lighting conditions for the Middlebury *Aloe* stereo dataset [HS07]. It provides seven views taken under three different lighting conditions and three different exposure times. We selected *view 0 illumination 1 exposure 1* and *view 1 illumi-*



Figure 6: View synthesis based on the scene in figure 5. Both syntheses are composed from the left image of figure 5 on the left of the red line and from the right image on the right of the red line. The synthesis on top is based on the synthetically deviated colors and the synthesis on the bottom is performed after a correction with our registration algorithm.

nation 2 exposure 1 for our evaluation as illustrated in figure 8. The color registration function is chosen according to section 5.2. Despite the very different lighting conditions the outcome of our registration algorithm is visually quite appealing as can be seen in figure 9. The view synthesis based on the original images clearly suffers from inconsistent colors while the synthesis after photometric registration looks very natural. Analogously to section 7.2, we additionally inspect the impact of our registration process on the disparity estimation in the geometric registration step as illustrated in figure 10. Likewise to section 7.2 the outcome clearly improves after applying our joint photometric and geometric registration process.

8. Conclusion

In this paper we presented a novel method for high accuracy joint photometric and geometric stereo image registration. We proposed a consistent, elegant and efficient real-time capable optimization framework based on an energy formulation of the registration problem. Our work extends the variational formulation for disparity estimation presented in [PSG*08] with regard to improved color insensitivity and robustness. Beside off-line postprocessing of stereo images, it can be seen as a valuable algorithm for the on-line setup



Figure 7: Disparities obtained from the globally optimal geometric image registration step. Top: Result for uncorrected colors. Bottom: Result after registration with the proposed method.



Figure 8: Images from the Middlebury Aloe dataset. Left: Aloe view 0 illumination 1 exposure 1. Right: Aloe view 1 illumination 2 exposure 1.

of stereo cameras used for disparity estimation. Simultaneously, we were able to show in our experimental results, that the optimization procedure is directly linked to the performance of disparity estimation and the visual quality of multi-view view synthesis. The potential of our algorithmic development has been successfully demonstrated by the evaluation with two different applications and three different datasets.

References

[Bar08] BARTOLI A.: Groupwise geometric and photometric direct image registration. *Pattern Analysis and Machine Intelligence, IEEE Transactions on* 30, 12 (2008), 2098–2108. 2

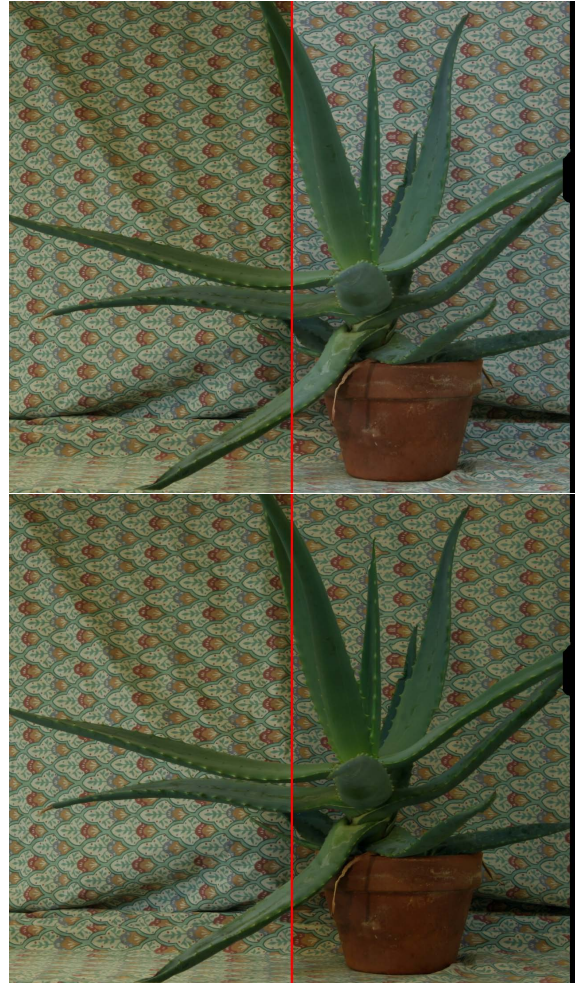


Figure 9: View synthesis based on the scene in figure 8. Both syntheses are composed from the left image of figure 8 on the left of the red line and from the right image on the right of the red line. The synthesis on top is based on original colors and the synthesis on the bottom is performed after a correction with our registration algorithm.

[CSZ09] CHAKRABARTI A., SCHARSTEIN D., ZICKLER T.: An empirical camera model for internet color vision. In *British Machine Vision Conference (BMVC 2009)* (London, UK, 2009). 2

[FSC98] FINLAYSON G. D., SCHIELE B., CROWLEY J. L.: Comprehensive colour image normalization. In *Proceedings of the 5th European Conference on Computer Vision-Volume I - Volume 1* (London, UK, 1998), ECCV '98, Springer-Verlag, p. 475–490. ACM ID: 649067. 2

[GN03] GROSSBERG M. D., NAYAR S. K.: Determining the camera response from images: What is knowable? *IEEE Transactions on Pattern Analysis and Machine Intelligence* 25, 11 (2003), 1455–1467. 2

[HLL08] HEO Y. S., LEE K. M., LEE S. U.: Illumination and camera invariant stereo matching. In *Computer Vision and*

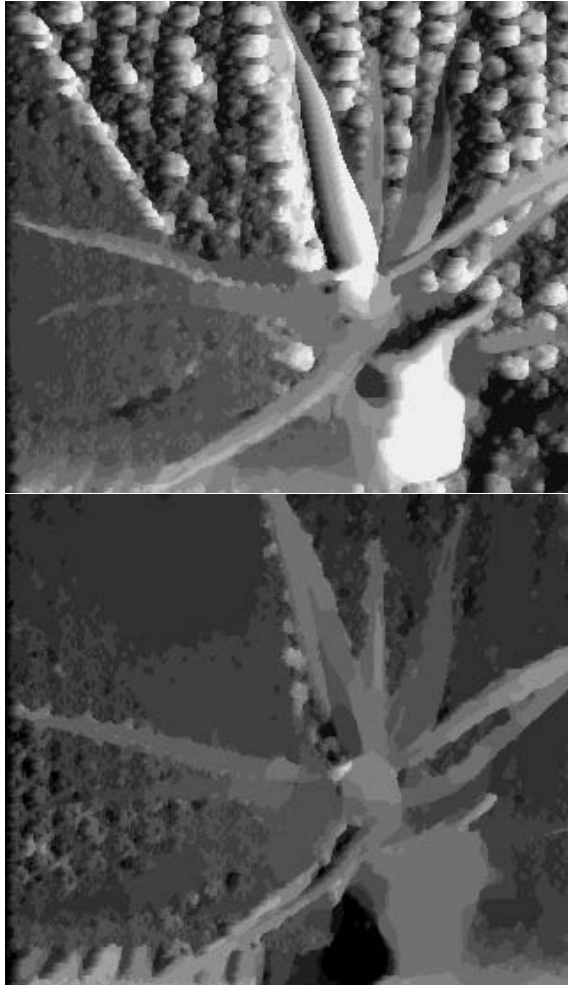


Figure 10: Disparities obtained from the globally optimal geometric image registration step. Top: Result for original colors. Bottom: Result after registration with the proposed method.

Pattern Recognition, 2008. CVPR 2008. IEEE Conference on (2008), pp. 1–8. [2](#)

- [HS07] HIRSCHMULLER H., SCHARSTEIN D.: Evaluation of cost functions for stereo matching. In *CVPR07* (2007), pp. 1–8. [1](#), [2](#), [6](#)
- [HS09] HIRSCHMÜLLER H., SCHARSTEIN D.: Evaluation of stereo matching costs on images with radiometric differences. *IEEE Transactions on Pattern Analysis and Machine Intelligence* 31, 9 (2009), 1582–1599. [1](#), [2](#)
- [IW05] ILIE A., WELCH G.: Ensuring color consistency across multiple cameras. In *Computer Vision, 2005. ICCV 2005. Tenth IEEE International Conference on* (2005), vol. 2, pp. 1268–1275 Vol. 2. [2](#)
- [KFP08] KIM S. J., FRAHM J., POLLEFEYS M.: Radiometric calibration with illumination change for outdoor scene analysis. In *Computer Vision and Pattern Recognition, 2008. CVPR 2008. IEEE Conference on* (2008), pp. 1–8. [2](#), [4](#)

- [KP08] KIM S. J., POLLEFEYS M.: Robust radiometric calibration and vignetting correction. *Pattern Analysis and Machine Intelligence, IEEE Transactions on* 30, 4 (2008), 562–576. [2](#), [4](#)
- [KSP*10] KETTERN M., SCHNEIDER D. C., PRESTELE B., ZILLY F., EISERT P.: Automatic acquisition of Time-Slice image sequences. In *Visual Media Production, Conference for* (Los Alamitos, CA, USA, 2010), vol. 0, IEEE Computer Society, pp. 40–48. [2](#)
- [PSG*08] POCK T., SCHOENEMANN T., GRABER G., BISCHOF H., CREMERS D.: A convex formulation of continuous Multi-Label problems. In *European Conference on Computer Vision (ECCV)* (Marseille, France, Oct. 2008). [3](#), [6](#)
- [RSYD05] RAMANATH R., SNYDER W., YOO Y., DREW M.: Color image processing pipeline. *Signal Processing Magazine, IEEE* 22, 1 (2005), 34–43. [2](#)
- [SFA*08] SCHREER O., FELDMANN I., ATZPADIN N., EISERT P., KAUFF P., BELT H.: 3DPresence -A system concept for Multi-User and Multi-Party immersive 3D videoconferencing. In *Visual Media Production (CVMP 2008), 5th European Conference on* (2008), p. 1–8. [1](#), [5](#)
- [WASF11] WAIZENEGGER W., ATZPADIN N., SCHREER O., FELDMANN I.: Patch-Sweeping with robust prior for high precision depth estimation in real-time systems. In *Proc. International Conference on Image Processing (ICIP 2011)* (Brussels, Belgium, 2011). [1](#), [5](#)
- [WFS11] WAIZENEGGER W., FELDMANN I., SCHREER O.: Real-time patch sweeping for high-quality depth estimation in 3D videoconferencing applications. In *Proc. of Real-Time Image and Video Processing* (San Francisco, California, United States, 2011). [1](#), [5](#)
- [WYD07] WANG L., YANG R., DAVIS J. E.: BRDF invariant stereo using light transport constancy. *IEEE Transactions on Pattern Analysis and Machine Intelligence* 29, 9 (2007), 1616–1626. [2](#)
- [ZMEK10] ZILLY F., MUELLER M., EISERT P., KAUFF P.: Joint estimation of epipolar geometry and rectification parameters using point correspondences for stereoscopic TV sequences. In *3DPVT10* (2010). [2](#)